Microchemical Journal 195 (2023) 109472

Contents lists available at ScienceDirect

Microchemical Journal

journal homepage: www.elsevier.com/locate/microc

Dental proteomic analyses and Raman spectroscopy for the estimation of the biological sex and age of human remains from the Greek cemetery of San Giorgio Extra, Reggio Calabria (Italy)

Enrico Greco [a,*], Andrea Maria Gennaro [b], Dario Piombino-Mascali [c], Daniela Costanzo [d], Simona Accardo [e], Sabina Licen [a], Pierluigi Barbieri [a], Stefano Fornasaro [a], Sabrina Semeraro [a], Elia Marin [f], Sara Signoretti [g], Caterina Gabriele [g], Marco Gaspari [g]

[a] Department of Chemical and Pharmaceutical Sciences, University of Trieste, Italy
[b] Italian Ministry of Culture (MiC), Superintendence of Reggio Calabria and Vibo Valentia, Italy
[c] Department of Anatomy, Histology and Anthropology, Vilnius University, Lithuania
[d] Italian Ministry of Culture (MiC), National Archaeological Museum of Reggio Calabria, Italy
[e] Aspasia Archaeoservice, Reggio Calabria, Italy
[f] Department of Materials Chemistry, Kyoto Institute of Technology, Japan
[g] Research Centre for Advanced Biochemistry and Molecular Biology, Department of Experimental and Clinical Medicine, Magna Graecia University of Catanzaro, Italy

A B S T R A C T

Sex and age estimation is one of the most fundamental steps in mortuary studies and bioarchaeology. It is essential for a deeper understanding of ancient societies, and has wide applications in gender archaeology. The aim of this paper is to create a new and reliable protocol for unambiguous sex estimation of the deceased, comparing proteomic analyses, archaeological evidence, and anthropological data from a Greek cemetery located in Reggio Calabria (or the ancient *Rhegion*), as well as a first approach to estimate the age of the deceased by Raman spectroscopy in archaeology. Excavations carried out in the San Giorgio Extra district, headed by the Superintendence for the Archaeological Heritage of Calabria during the years 2004 and 2007, led to the discovery of the most significant Hellenistic cemetery in the city. Specifically, archaeological campaigns brought to light thirty Greek inhumation burials and their related funerary objects. Through proteomic analyses, we monitored a total of eight characteristic peptides for the amelogenin isoform variants AMELX and AMELY from the dental enamel of twelve selected adult individuals. The presence or absence of the AMELY variant (exclusively present in male subjects, being encoded by the Y gene) allowed us to estimate the sex of the analyzed individuals with high accuracy. Raman spectroscopy was also applied to study the enamel and dentin crystallinity to determine other environmental and biological parameters. At the same time, archaeological studies based on artifacts discovered inside the graves and double-blind bio-anthropological sex estimation of the twelve subjects were performed in order to compare these evaluations with data from the proteomic analyses. Comparison between these different approaches produced totally congruent results for the majority of individuals. In addition, the proteomic analysis allowed us to estimate the sex of four poorly preserved subjects for whom sex estimation was somewhat doubtful, as well as that of one undetermined individual. Finally, proteomic results were produced here with a faster protocol than those found in the literature and are potentially scalable to much lower sample amounts.

1. Introduction

Methodological advancements in the field of protein analysis have brought about a profound transformation in the range and diversity of applications, including within the realm of archaeology. Within this emerging field of study, numerous applications have been utilized to examine archaeological materials and remains in recent years [1]. These analyses have been employed to discern between sheep and goat specimens, gain insights into past ecologies and environments, and shed light on ancient cuisine and culinary practices [2,3]. More recently, considerable attention has been drawn toward the preservation of amelogenin, an enamel protein encoded by genes located on the X and Y chromosomes. Due to variations in the protein sequences of amelogenin between its X and Y variants, this protein can serve as a marker for biological sex [4].

The estimation of biological sex constitutes a critical factor in the archaeological reconstruction of ancient societies. However, this process can be subjected to biases and challenges, particularly concerning the preservation state of the skeletons. Typically, this estimation relies on classical and geometric morphometric approaches [5], while

* Corresponding author.
E-mail address: enrico.greco@units.it (E. Greco).

https://doi.org/10.1016/j.microc.2023.109472
Received 14 June 2023; Received in revised form 25 September 2023; Accepted 3 October 2023
Available online 6 October 2023

archaeologists often turn to gender-associated funerary objects, potentially leading to misconceptions regarding the social role, status, and relationship of the individual with the community [6,7]. Through proteomic analyses, we are now able to obtain more reliable results in estimating the sex of the analyzed individuals. The dataset utilized for our investigation originates from the ancient city of *Rhegion* (Reggio Calabria), where archaeologists have excavated the San Giorgio Extra cemetery. This dates back to the Hellenistic and Republican periods (i.e., 4th-2nd centuries BCE). All of the evidence was subjected to three independent methods of gender and sex estimation (archaeological, proteomic, and osteological) and Raman spectroscopy for age estimation, enabling comparisons and cross-validation of techniques.

2. The archaeological context: The necropolis of San Giorgio Extra

In 2004, the former Superintendence for the Archaeological Heritage of Calabria conducted rescue excavations at a construction site in the San Giorgio Extra area of Reggio Calabria. These excavations revealed a section of the southern necropolis of *Rhegion*, situated between 6 and 9 m below the road surface [8]. Despite being hampered by structural issues, the excavation proved to be of utmost significance for the reconstruction of the topography of ancient Greek Reggio. It enabled the identification of the southernmost boundary of the ancient city, which had until then been purely speculative. Knowledge regarding Reggio's cemeteries was also quite limited and uncertain, with the exception of some archaic discoveries in the area of Santa Caterina [8]. The archaic and classical tombs of the city were largely unknown, while those from the Hellenistic and Roman periods were better documented. The findings at San Giorgio Extra can be attributed to the Hellenistic/Republican phase [8].

A total of thirty-two tombs were identified during the initial excavation campaign, with some of them overlapping due to their varying depths. Chronologically, they fall into four different phases spanning the 4th – 2nd century BCE. Architecturally, these tombs exhibit previously documented typologies in Reggio. Among them are five "*copertura a libro*" (book-roofed) tombs, seven cyst tombs covered with a flat roof consisting of three or four layers of large tiles forming a false vault, three tombs covered with three or four clay semi-rings (similar to those used in constructing wells during the Greek period), ten "*cappuccina*-tombs" (tombs built with tiles), and four box tombs with sloping brick roofs. Additionally, two simple pit burials, two *ustrina* (burial areas for cremated remains) containing bone fragments and burnt objects (such as clay miniature capitals, clay balsam jars, cups, and lids), and two incinerations in jars were discovered. These findings indicate the coexistence of both incineration and inhumation practices during the Hellenistic period.

In order to provide a better understanding of the graves and grave goods directly investigated within our research, we will now present an analytical description of the burials from which our samples were obtained. Grave no. 21 is a *cappuccina*-tomb, while graves no. 7 and 9 belong to the category of cyst tombs with pitched roofs (see Fig. 1).

Graves no. 16 and 26 are simple pit burials with book covers, and grave no. 29 is the only example of a cyst tomb with a book cover. Graves no. 8, 19 (see Fig. 2), and 20 are instances of cyst tombs with flat false vault covers, while graves no. 28 and 30 cannot be classified due to their poor state of preservation (possibly belonging to the *cappuccina* type).

A predictive analysis of biological sex based on the culturally estimated gender of the adult deceased was also conducted. This focused on the grave goods found in twelve burials belonging to adult individuals for which proteomic analysis was feasible. Initially, we relied solely on the archaeological approach to make an educated guess about the possible biological sex [6], without considering the osteological evaluation and the definitive results from the proteomic method. Subsequently, with a postdictive approach, we compared the results derived from archaeological assessment, proteomic-based estimations, and osteological data. By aligning the findings from these three different approaches, we intended not only to evaluate specific instruments and techniques but also to explore mortuary patterns and engage in theoretical discussions regarding methodological implications in mortuary archaeology in general, and specifically in the Greek period of Southern Italy.

2.1. Archaeological predictive approach to biological sex estimation

Archaeological science has played a significant role in determining various aspects of the social identity of the deceased, including their age, gender, social status, and the position of their tomb. The study of the material assemblages found within funerary contexts is crucial for comprehending the social organization of a particular society and, more specifically, for speculating on the presumed biological sex (as opposed to the archaeological gender based on grave goods) or the age of the deceased. Traditionally, necklaces or jewelry typically suggest a female individual, while swords or weapons indicate a male individual. However, it is important to note that there are exceptional cases and, as we

Fig. 1. Grave no. 7.

Fig. 2. Grave no. 19.

will see in the burials discussed here, the dichotomy is much more nuanced, and interpretations of the collected evidence are not always straightforward.

In general, the grave goods discovered in the cemeteries of San Giorgio Extra conform to the typologies already known in the city of the Messina Strait. Alongside a significant quantity of clay artifacts, particularly *unguentaria* and painted clay miniature capitals (which are distinctive elements of the Reggio necropolis and are usually placed as ornaments at the four corners of the funerary bed), a wide variety of ceramic vessels, predominantly in black paint, have been unearthed (Table 1). Several bronze objects have also been found, including an intact mirror, glass paste *alabastra*, a pair of golden earrings in the shape of an antelope's head, and an Egyptian scarab seal ring. Of particular interest are thin gold disks of various sizes, discovered inside the mouths of some skeletons. Known as *bracteae* in the archaeological literature, these disks are adorned with scenes, though they are not always easily legible and are traditionally referred to as "Charon's offerings".

Regarding our study on funerary assemblages, we have identified certain objects as markers that allow us to reasonably infer the biological sex of the deceased. Notably, the presence of jewelry such as earrings and a ring in tomb no. 28 (see Fig. 3), as well as mirrors in tombs no. 28 and 19, and rouge in tomb no. 19, are considered indicators of female burials.

Additionally, the discovery of a terracotta doll and forceps in tomb no. 30 (see Fig. 4) further reinforces the identification of a female burial.

On the other hand, markers related to male burials are less apparent, with the exception of an unidentified bronze object found in tomb no. 9. Unfortunately, the proteomic investigation could not be conducted on the burials containing a sword blade and a riding stirrup. The interpretation of the golden *bracteae* remains inconclusive, as their meaning cannot be definitively estimated. The same assessment applies to the more commonly found pottery shapes, particularly *unguentaria* and cups, which were discovered without a clear connection to the possible age or biological sex of the deceased. These vessels are closely associated with Greek funerary rituals and were used to contain perfumed oils, which were also applied to the body, or offerings of food and liquids.

Finally, the presence of a terracotta doll in tomb no. 30 raises important questions regarding the estimation of the age at death. The so-called "doll" is a widespread finding of terracotta during the Archaic and Classical periods. The presence of this peculiar item has been interpreted by archaeologists in two different ways: while some consider it a simple toy due to its movable limbs, others emphasize its religious and funerary value. The doll wears a cap, and its peculiar iconography shows a close parallel with representations of Attis, a Phrygian deity connected with Cybele. Interpretations of this item remain problematic.

2.2. Postdictive archaeological approach to biological sex estimation

We have provided a brief overview of the material assemblages discovered in the twelve Hellenistic-Republican burials that were analyzed. We also attempted to estimate the biological sex of the deceased based solely on their inferred gender, which was derived from archaeological evidence (grave goods). Now, we will alter the typical research approach by starting with the definitive data obtained from the results of the proteomic analysis. Subsequently, by comparing these data with the assumptions made in the previous section, we will be able to examine the agreements and disagreements between each method, both in terms of definitive and conditional estimates. This postdictive approach can be regarded as a validation test of the archaeological inferences related to our specific site and material evidence [9].

It is important to note that this analysis was conducted on a limited sample of cases, which we believe is still valuable to highlight certain trends and tendencies. Despite the inherent limitations in sample size, our analysis serves as a model for future researchers who wish to apply theoretical assumptions, either to confirm or refute our conclusions [10]. The results of this data comparison are summarized in Table 2.

As indicated, a total of twelve burials belonging to adult individuals were analyzed; however, tomb no. 21 did not yield a funerary assemblage, preventing any hypotheses of gender from being made. For tombs no. 16 and 26, the presence of a deceased male was suggested based on the discovery of an iron fibula in both graves. This initial assumption was subsequently confirmed through postdictive verification. The initial attribution of the female sex to the deceased in burials no. 7 and no. 8 was also validated, despite tomb no. 7 yielding an iron fibula as well. For burial no. 15, which was considered a likely female burial due to the presence of a golden *bractea*, conflicts arose from the proteomic analysis. As previously mentioned, it is methodologically incorrect to consider this category of artifacts as a definitive indicator of differentiation between the two sexes, unlike items such as jewelry or mirrors that are typically associated with female burials. It is important to note that the presence of *bombylios*, a specific type of pottery shape, is exclusive to female burials. Further systematic research and comparative analysis are required to address this hypothesis more comprehensively.

3. Methods

For proteomic analyses, the samples were processed according to the procedure outlined by Lugli et al. [4]. Tooth samples were first cleaned with HPLC water, and enamel chunks weighing 10–50 mg were washed three times. The first cycle involved an ultrasonic bath with HPLC water, followed by a 5-minute incubation with 1 M HCl, and a final washing step with HPLC water. To extract enamel proteins, the specimens were

Table 1
The twelve graves analyzed.

GRAVE no.	GRAVE TYPOLOGY	FUNERARY ASSEMBLAGE	GENDER ESTIMATION
7	Book-roofed	1. Black glazed cup 2. Iron fibula	Male (uncertain)
8	Flat-roofed	1. Cup 2. *Lekythos* or *unguentarium*	Female (uncertain)
9	Tile-built ("*a cappuccina*")	1. Bone studs (3) 2. Small cup 3. *Unguentarium* 4. Bronze item	Male
15	Tile-built ("*a cappuccina*")	1. Golden *bractea* 2. Black glazed cup Outside: ● *Alabastron* ● *Unguentarium* ● Terracotta flower	Female (uncertain)
16	Book-roofed	1. *Unguentaria* (3) 2. Small black glazed cup 3. Iron *fibula* (brooch) 4. Nails	Male (uncertain)
19	Flat-roofed	1. *Pyx* (fragments) 2. *Lekane* (fragments) 3. Bronze medallion 4. Vitreous *olpe* 5. *Unguentaria* (9) 6. Black glazed *bombylios* 7. Ovoid bottle 8. Flask 9. Shells and beauties	Female
20	Flat-roofed	1. *Unguentaria* (3) Outside: ● *Pyx* ● Black glazed *bombylios*	Female
21	Tile-built ("*a cappuccina*")	//	Undefined
26	Book-roofed	1. Iron *fibula* (brooch) 2. Small *olpe* 3. Nails	Male (uncertain)
28	Tile-built (possibly "*a cappuccina*")	1. Golden earrings 2. Golden *bractea* 3. Scarab ring 4. Bronze mirror 5. *Alabastron* 6. *Unguentaria* (3) 7. Small cup 8. Nail 9. Animal-shaped *protome* (cow?) Outside: ● Bull-shaped *protome*	Female
29	Book-roofed	I: 1. Iron nails (15) 2. Bronze nail 3. Bronze medallion 4. *Unguentaria* (4) 5. Small cup II: 1. Pin 2. *Fibula* (brooch) 3. *Unguentaria* (14) 4. Small black glazed cups (2) 5. Black glazed *bombylios* 6. Iron nails 7. Blades (2)	Female
30	Tile-built (possibly "*a cappuccina*")	1. *Alabastron* 2. *Alabastron* (fragment of foot) 3. Cup 4. *Forceps* (fragment)	Female

Table 1 (*continued*)

GRAVE no.	GRAVE TYPOLOGY	FUNERARY ASSEMBLAGE	GENDER ESTIMATION
		5. *Unguentarium* 6. Terracotta mortar 7. Small black glazed cup 8. *Pyx* 9. Terracotta doll	

Fig. 3. Pottery (a, c) and golden earrings (b) from tomb no. 28.

Fig. 4. Terracotta doll from tomb no. 30.

Table 2
Postdictive comparison between archaeological, osteological, and proteomic biological sex estimation.

GRAVE no.	GRAVE TYPOLOGY	ARCHAEOLOGY-BASED GENDER EVALUATION	OSTEOLOGY-BASED BIOLOGICAL SEX ESTIMATION	PROTEOMIC-BASED BIOLOGICAL SEX IDENTIFICATION
7	Book-roofed	Male (uncertain)	Female (possible)	Female
8	Flat-roofed	Female (uncertain)	Female (possible)	Female
9	Tile-built ("*a cappuccina*")	Male	Male	Male
15	Tile-built ("*a cappuccina*")	Female (uncertain)	Female (possible)	Male
16	Book-roofed	Male (uncertain)	Male	Male
19	Flat-roofed	Female	Undetermined	Female
20	Flat-roofed	Female	Female	Female
21	Tile-built ("*a cappuccina*")	Undefined	Female	Female
26	Book-roofed	Male (uncertain)	Male (possible)	Male
28	Tile-built (possibly "*a cappuccina*")	Female	Female (possible)	Female
29	Book-roofed	Female	Female	Female
30	Tile-built (possibly "*a cappuccina*")	Female	Female	Female

soaked in 1 M HCl with a ratio of 1:20 (weight/volume) for 3 h at room temperature in a glass vial. The extracted peptides were then purified through StageTip purification, as described by Taverna and Gaspari [11]. In brief, each sample was first diluted with 0.1 % TFA and then purified with C18 StageTips. The peptides were loaded into the StageTip and washed with 0.1 % TFA before being eluted with water and acetonitrile (1:1 ratio). The eluate was then diluted 15-fold in mobile phase A, which was subsequently injected for nanoLC-MS/MS analysis (2 μL).

The nanoLC analysis was conducted according to the methodology outlined by Taverna and Gaspari [11]. A Thermo Fisher Scientific EasyLC 1200 instrument was employed for chromatography, which was coupled to a Q-Exactive "traditional" mass spectrometer (Thermo Fisher Scientific). The nanoLC column was a pulled capillary with dimensions of 0.075x130 mm (i.d. and column length, respectively) and was packed in-house with C18 silica particles obtained from Dr. Maisch. Peptides were loaded on-column directly at a flow rate of 500 nL/min in mobile phase A (consisting of 2 % acetonitrile and 0.1 % formic acid) and eluted at 230 nL/min through a linear gradient. The gradient started with 10 % B and increased to 50 % B over 20 min. Additionally, there was a 5-minute ramp to 100 % B, followed by a 5-minute column regeneration at 100 % B. Mobile phase B was composed of 80 % acetonitrile and 0.1 % formic acid (v/v). Peptides were electrosprayed in positive ion mode at a spray voltage of 1800 V. MS acquisition was conducted using a mixed data-dependent acquisition/parallel reaction monitoring (DDA/PRM) approach. A full MS1 spectrum (resolution 35,000, scan range 350–1000 *m/z*) was followed by six data-dependent MS2 scans (top-6), with 6 s of dynamic exclusion. Subsequently, eight consecutive precursors were monitored using PRM mode (refer to Table 2). All MS2 events had a maximum injection time of 60 ms, a resolution of 17,500, an isolation window of 1.6 *m/z*, and a collision energy of 25 in normalized units.

The raw data obtained from DDA were subjected to a search using three databases: Swiss-Prot (restricted to *Homo sapiens*), an in-house database from UniProt containing mammal amelogenin sequences, and cRAP for contaminants. The search parameters did not include any proteolytic enzyme, and variable modifications such as deamidated asparagine/glutamine (NQ) and oxidized methionine (M) were set. The mass tolerances were 10 ppm for precursor ions and 0.05 Da for fragmented ions. An automatic decoy database was used to estimate the false discovery rate, with a probability threshold set at FDR < 1 %. For a protein to be considered identified, at least two unique peptides were required. To analyze the PRM data, specific extracted ion chromatograms were constructed for each monitored precursor using Xcalibur software with a mass tolerance of 50 ppm. To generate extracted ion chromatograms from the full-scan MS data of seven AMELX peptides, a tolerance of 10 ppm was applied. Peak areas were manually integrated using Xcalibur and were employed for probability estimation in the case of females.

For the Raman experiments, a Horiba T64000 spectrometer (Horiba, Kyoto, Japan) equipped with a 100x optical lens and an 1800 gr/mm grating was utilized. By the use of a triple monochromator, the spectral resolution was close to 0.1 cm^{-1}. All spectra were obtained with a 488 nm laser source, the exposition time varying between 2 s and 10 s depending on the intensity of the signal and the sample's background fluorescence. For each area of each specimen, 10 measurements were performed at randomized locations. The spectra were then averaged and normalized with respect to the band located at about 960 cm^{-1} and related to phosphate.

The biological sex of each individual had already been macroscopically assessed at the museum. According to a traditional biological anthropology approach, some bones such as the skull and pelvis can provide accurate indications for biological sex estimation. Therefore, specific features of those bones were observed, including the nuchal crest, mastoid process, supraorbital margin, glabella, mental eminence, and shape of the greater sciatic notch. Each trait was assigned a score on a scale of 1 to 5, representing female, possible female, undetermined, possible male, and male, respectively [5]. The overall morphology of the pelvis, taking into account features such as the preauricular sulcus, subpubic angle, and those first described by Phenice (ventral arch, subpubic concavity, and medial aspect of the ischiopubic ramus), was also considered. All of the individuals examined in this study had reached puberty and displayed skeletal characteristics associated with adulthood [5].

4. Results

Through osteological examination of the twelve adult individuals, five were identified as female, three as possible females, two as males, one as a possible male, and one as undetermined due to poor preservation (see Table 2). The classification of sex as "possible" was attributed to the absence or inadequate preservation of some specific traits.

To estimate the biological sex by analyzing the enamel proteins, we focused on the detection of two amelogenin peptides, SM(ox)IRPPY (AMELY) and (AMELY; [M+2H] + 2 440.2233 *m/z*) and SIRPPYPSY (AMELX; [M+2H] + 2 540.2796 *m/z*), which were previously shown to be abundant in enamel matrix [4,12]. We also searched for additional peptides listed in Table 3 to confirm the presence or absence of AMELY. These peptides were identified by searching the DDA data against our databases.

Upon analyzing the ion chromatograms, we found that the AMELX peptide SIRPPYPSY was present in all samples. However, the AMELY peptide SM(ox)IRPPY, along with three other AMELY peptides monitored, were only found in four out of twelve individuals (Fig. 5): T9, T15, T16, and T26 (complete results for AMELY negative chromatogram in Supplementary materials). Our database searches also revealed the presence of other tooth proteins, including CO1A1 (collagen type I α1),

Table 3
Precursors monitored in PRM scans. Fragment ions used for producing extracted ion chromatograms (XICs) are also reported.

m/z precursor	Gene name	Peptide sequence	Fragments used for XICs
440.22	AMELY	SMoxIRPPY	154, 408.2, 645.4
396.71	AMELY	MoxIRPPY	364.7, 655.3
432.22	AMELY	SMIRPPY	143.1, 191.1, 645.1
483.74	AMELY	SMoxIRPPYS	451.7, 732.4
540.28	AMELX	SIRPPYPSY	366.1, 686.3, 714.4
525.30	AMELX	SYEVLTPLK	223.1, 357.2, 670.4, 799.5
423.22	AMELX	MPLPPHPG	104.1, 504.2, 714.4
431.22	AMELX	MoxPLPPHPG	504.2

CO1A2 (collagen type I α2), and DSPP (dentin sialophosphoprotein), which may have been due to residual dentin tissue. Our search on the cRAP database did not identify any evidence of modern contaminants. To estimate the probability of accurate assignment for female samples, we employed the formula proposed by Parker et al. [13] To do so, we determined the area of extracted ion chromatograms for seven primary AMELX peptides (selected based on their frequency of detection in DDA) and utilized these data for probability estimation. Given that the signal from AMELX peptides was consistently robust, all probabilities exceeded the 95 % threshold as indicated in Table 4 and Fig. S1–S8.

Fig. 6 shows the average Raman spectra obtained from the dentin region of the different samples. Despite the similarities between samples from different burial sites, the average spectra present major differences when compared to recently explanted teeth [14], in particular concerning the intensity of the bands related to amides, which are the basic units that form collagenous tissues. In Fig. 5, bands related to Amide I, Amide III, and CH_2 bending in organic molecules are barely detectable and much broader than previously reported in the literature [15] for similar experimental conditions, suggesting that the organic fraction of dentin, which essentially consists of collagen fibers, degraded over time even when not directly exposed to the external environment. Moreover, fluctuations in the relative intensity of the v_4 PO_4^{3-}/v_1 CO_3^{2-} vibration modes at about 1050–1080 cm^{-1} when compared to v_1 PO_4^{3-} suggest different degrees of carbonate substitutions between samples, A-type in particular [16]. Higher contents of A-type carbonate substitutions have previously been correlated with old age [17], but never for archaeological samples.

Based on the relative intensity of the A-type substitution band at about 1080 cm^{-1} when compared to the band at about 1050 cm^{-1}, samples no. 8, 20, and 26 would seem to be coming from relatively young individuals, while all other samples seem to have a comparable relative intensity. Sample no. 28′s age could not be estimated with this method due to the presence of an unknown band located at about 1090 cm^{-1} that partially overlaps with v_1 CO_3^{2-}.

Fig. 7 shows the main spectroscopic parameters that could be obtained from the various dentin samples. The full-width at half maximum (FWHM) of the band located at about 960 cm^{-1}, and associated with v_1 PO_3^{4-} vibrations, can be used to estimate the crystallinity of the hydroxyapatite phosphate groups. In Fig. 7 (a), the blue band represents the average values from the literature obtained with similar experimental conditions on modern teeth. We can observe that for samples no. 7, 9, 16, 28, 29, and 30 the band is broader than the average, which indicates a lower degree of crystallinity.

Low crystallinity can be caused by many environmental and biological factors: studies have shown that dentin crystallinity in particular tends to decrease with age. This is thought to be due to the gradual replacement of the mineral component of dentin with organic material over time. As the collagen matrix becomes more dominant, the alignment and orientation of the hydroxyapatite crystals become less organized, resulting in a decrease in crystallinity [18]. A loss of crystallinity can also be caused by exposure to acidic environments [14], but dentin is, in most cases, less exposed than enamel and thus less influenced.

The Raman shift of the same band (Fig. 7 (b)) can be associated with many factors, from composition to residual stresses. It can be observed that in four cases, namely samples no. 15, 19, 29, and 30, the Raman shift was relatively high when compared to the reference, which indicates that the crystallographic structure of the apatite was distorted.

Fig. 7(c) shows the intensities of the sub-bands at about 945 cm^{-1}, related to carbonated substitutions [19,20] and 965 cm^{-1}, attributed mainly to carbonate substitutions at B-type sites [21] or to the presence of tri-calcium phosphate [22]. In samples no. 7, 16, 29, and 30 the 960 cm^{-1} band is broad, but the sub-bands are relatively weak, indicating a demineralization, possibly because of aging. Samples no. 8, 9, 15, 20, 21, and 26 on the other hand, seem to have high contents of carbonated substitutions, which have been previously correlated with lower tooth maturity and younger age [23].

It must be noted that the quality of the Raman spectra of dentin for sample no. 19 was especially poor, making results related to this sample less reliable.

Fig. 8 shows the average Raman spectra obtained from the enamel region of the different samples. When compared to dentin, the enamel is more exposed to the environment, and the relative Raman spectra are expected to be more influenced by other variables like mastication and diet. The overall collagen content in enamel is usually close to zero, as it is completely absorbed during the course of mineralization and maturation [24]. Nevertheless, weak, broad Raman bands can be spotted in the region between 1200 and 1300 cm^{-1}, associated with residual enamel proteins. As has been previously observed for dentin, those bands appear to be too weak and broad to be properly fitted and/or identified.

Notwithstanding the higher influence of environmental conditions, wear, and diet, the relative intensities of the band based on the relative intensity of the A-type substitution at about 1080 cm^{-1}, when compared to the band at about 1050 cm^{-1}, again show lower relative intensities for samples no. 8, 20, and 26, further supporting the hypothesis that those three samples could derive from younger individuals.

Despite showing a slightly higher relative intensity in dentin, the graph in Fig. 8 suggests that sample no. 30 could belong to a relatively young individual too, unlike the previously undetermined sample no. 28.

Fig. 9 shows the main spectroscopic parameters that could be obtained from the various enamel samples. When compared to dentin, the enamel is more exposed to the surrounding environment, subject to the aggression of pathogens and by the impact of mechanical damage caused by mastication. Thus, Raman spectroscopy investigations of enamel provide additional insights.

The full-width at half maximum of the band located at about 960 cm^{-1} and associated with PO_3^{4-} vibrations is particularly high for samples no. 9, 26, 28, and 30. With the exception of sample no. 26, these results are consistent with what was observed for dentin (Fig. 6(a)). Surprisingly, a few samples, namely no. 7, 8, 15, and 19 have significantly lower width values when compared to the reference, which might indicate that they were most likely affected by environmental conditions during burial [22,25], as values below 9 cm^{-1} are quite unusual for biological hydroxyapatite. It is interesting to note that sample no. 19, which was in the worst state of preservation and could not provide reliable Raman data for dentin (Fig. 7) also shows the highest degree of crystallinity.

Apart from crystallinity, Raman shift (Fig. 9(b)) was also monitored. Four samples, namely no. 15, 19, 21, and 28 showed a clear shift of the peak position to higher values. There is a clear correspondence with the results obtained for dentin only for samples no. 15 and 19, which indicates that the causes of the crystallographic distortions are different in the two materials.

Considering the combined results of Fig. 9(b) with the relative intensity of the sub-bands of Fig. 8(c), it can be observed that samples no. 15, 19, 21, and 28 have relatively intense sub-bands at 975 cm^{-1}. Sample no. 29, on the other hand, has the sub-band at 970 cm^{-1} as the most intense band, which explains why the values of the FWHM and the

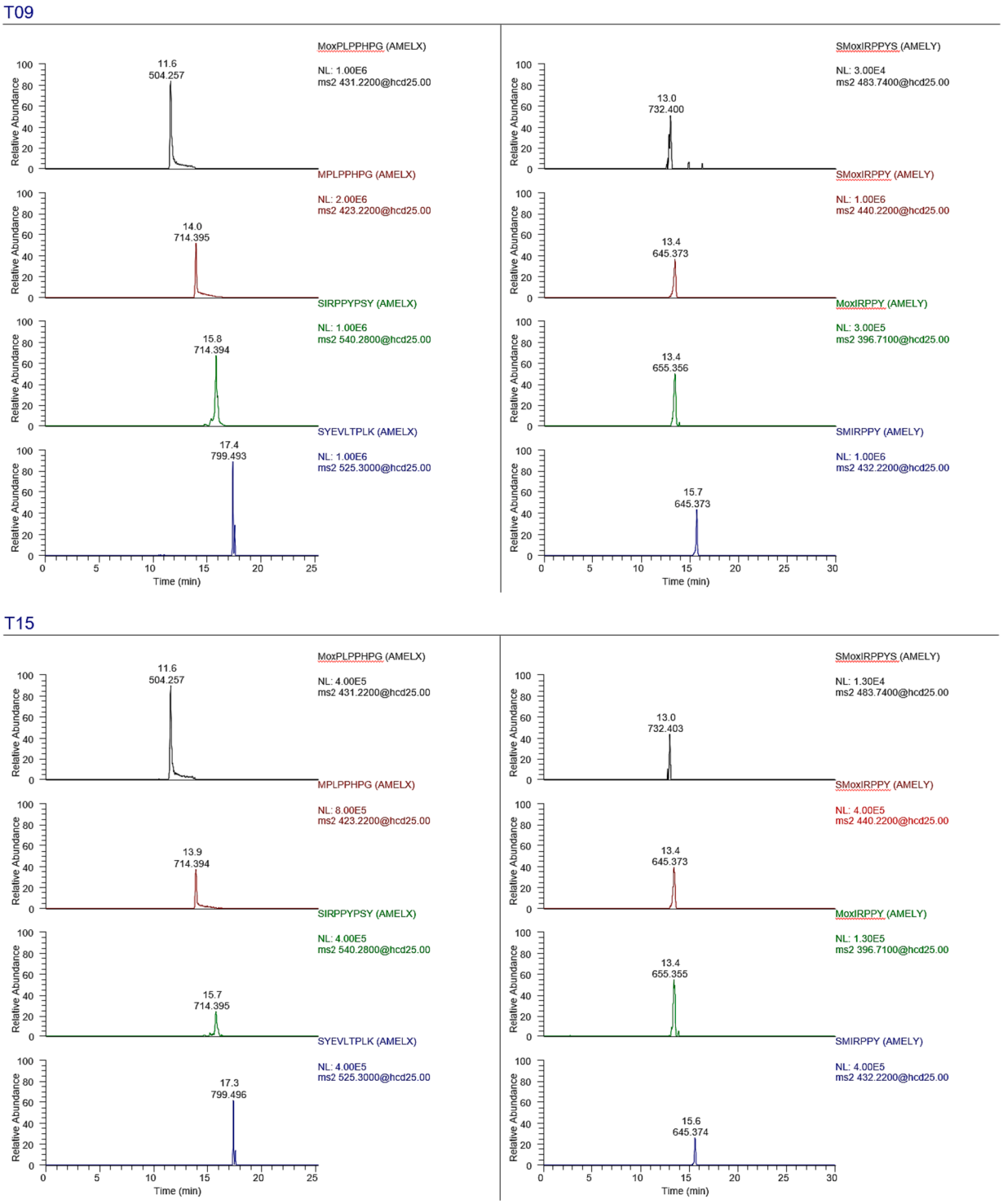

Fig. 5. Extracted ion chromatograms (XICs) for amelogenin peptides. Four different XICs monitoring AMELX peptides are displayed on the left panels for samples no. 9, 15, 16, and 26, whereas four different XICs monitoring AMELY peptides are displayed to the right. AMELX peptides (left) are monitored as positive controls. AMELY peptides (right) confirm the sex of these four samples (male). Precursor *m/z* and normalized ion count levels (NL) are displayed next to the corresponding XICs. Each ion count represents the sum of the intensities of fragment ions indicated in Table 3.

Raman shift of the band at 960 cm^{-1} are apparently normal. All five bands show clear signs of the presence of tri-calcium phosphates, possibly due to exposure to the environment during interment. It must be noted that, just like in dentin, carbonate content has been shown to decrease with age, but the contribution of carbonate to the Raman spectra can be influenced by environmental factors that do not affect dentin.

5. Conclusions

Our study has demonstrated that osteological sex estimation exhibits reliability and consistency with other techniques when dealing with

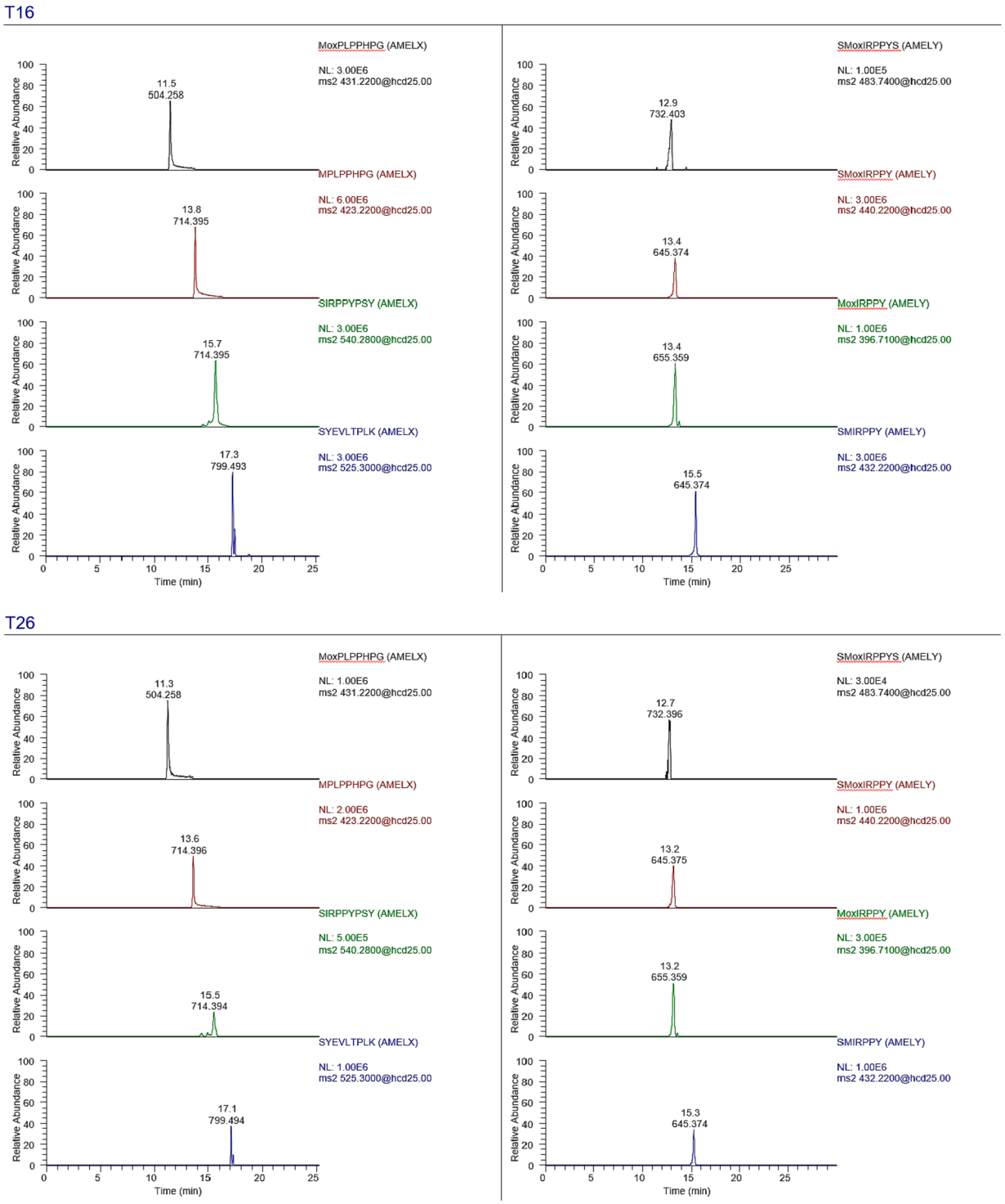

Fig. 5. (*continued*).

samples characterized by good preservation status. However, when assessing fragmentary and juvenile remains, it exhibits a substantial rate of indeterminate sex assignments. As noted in the study by Buonasera et al. [10], genomic methods may offer a potential avenue for extending sex estimation to numerous juvenile or fragmentary remains. Nevertheless, these methods exhibit a notable rate of conflicts with osteological or proteomic estimates, particularly when the conditional sex assignments fall below the threshold of 100,000 total mapped reads. Consequently, we opted to prioritize the proteomic method over the DNA-based approach.

Proteomic sex estimation emerged as the most sensitive technique in our analysis, consistently delivering results for all tested remains, with an average confidence level of 99.8 %. This remarkable accuracy can be attributed in part to the stability of the amelogenin peptide signal. However, it should be noted that the effectiveness of proteomic sex estimation is contingent upon the preservation of associated dentition within each burial context.

Proteomic analyses have provided us with more reliable estimations of biological sex for all twelve individuals, overcoming the limitations of morphological approaches that may have produced unreliable results.

Table 4
AMELX peptides identified with a high number of PSM (>10) in samples of interest. The area of the chromatographic peaks is also reported.

Sequence	Charge	*m/z*	RT	Area T07	Area T08	Area T19	Area T20	Area T21	Area T28	Area T29	Area T30
mPLPPHPGHPG	3	384,859	9,2	7,4E + 07	9,6E + 07	6,0E + 06	1,1E + 07	1,5E + 08	9,2E + 07	8,0E + 06	3,3E + 07
mPLPPHPGHP	3	365,852	9,4	2,2E + 07	2,9E + 07	2,0E + 06	0,0E + 00	3,8E + 07	2,9E + 07	0,0E + 00	0,0E + 00
mPLPPHPG	2	431,218	10,0	2,5E + 08	2,6E + 08	5,5E + 07	1,7E + 08	4,2E + 08	3,1E + 08	3,6E + 07	1,2E + 08
MPLPPHP	2	402,709	11,9	4,7E + 07	4,80E + 07	1,5E + 07	4,2E + 07	7,9E + 07	5,9E + 07	8,0E + 06	2,2E + 07
MPLPPHPGHPG	3	379,527	11,0	2,3E + 07	4,4E + 07	4,0E + 05	0,0E + 00	1,6E + 08	4,4E + 07	0,0E + 00	5,0E + 06
MPLPPHPG	2	423,221	12,5	9,8E + 07	1,4E + 08	1,9E + 07	2,4E + 07	4,5E + 08	1,4E + 08	8,0E + 06	1,8E + 07
SIRPPYPSY	2	540,279	14,1	7,0E + 07	8,9E + 07	0,0E + 00	1,0E + 06	2,0E + 08	6,3E + 07	0,0E + 00	2,5E + 06
			SUM	**5,9E + 08**	**7,0E + 08**	**9,7E + 07**	**2,5E + 08**	**1,5E + 09**	**7,4E + 08**	**6,0E + 07**	**2,3E + 08**
			mg of enamel injected on column (2/150*1/20 = 1/1500 of max 50 mg)	**3,3E-02**	**3,3E-02**	**3,3E-02**	**3,3E-02**	**3,3E-02**	**3,3E-02**	**3,3E-02**	**3,3E-02**
			% probability	**99,2**	**99,3**	**97,0**	**98,5**	**99,6**	**99,3**	**95,7**	**98,4**

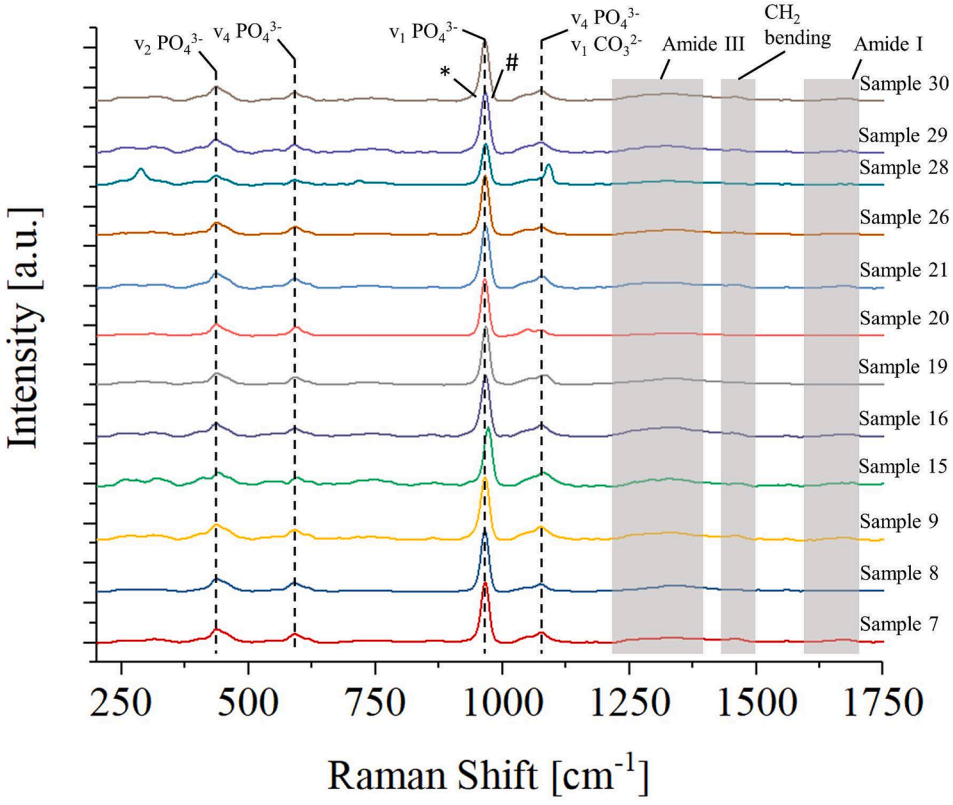

Fig. 6. Average Raman spectra as obtained on the dentin regions of the different specimens. Phosphate's main vibration modes and regions related to Amide vibrations are marked. Sub-bands at 945 and 975 cm^{-1} and related to distorted structures of PO_4^{3-} or CO_3^{2-} are marked with "*" and "#".

This has significantly contributed to our understanding of the demographic composition of the individuals buried in the necropolis. The value of combining three different and complementary approaches became evident when variations in mortuary treatments and preservation restricted the efficacy of a single method. Proteomics proved particularly useful in estimating sex in cases where the archaeological study faced limitations due to various factors. However, it is important to note that only twelve out of 30 graves contained teeth with sufficient enamel for analysis, which constrained the application of proteomic techniques. On the other hand, archaeological evidence was available for 28 out of 30 tombs, but as previously mentioned, only a small portion of the funerary assemblages provided specific indications regarding the possible biological sex of the deceased, which was essentially assumed based on the gender association of the artifacts included in the burials. However, the findings of this study demonstrate disparities in Raman spectroscopy results between archaeologically retrieved teeth and recently explanted ones, specifically indicating a minimal presence of residual collagen in the former. This variation in collagen content can be attributed to disparate environmental conditions that the teeth have encountered throughout their exposure period, and even dentin, which is usually not directly exposed to the environment, was degraded to the point that spectroscopic markers associated with collagenous tissues

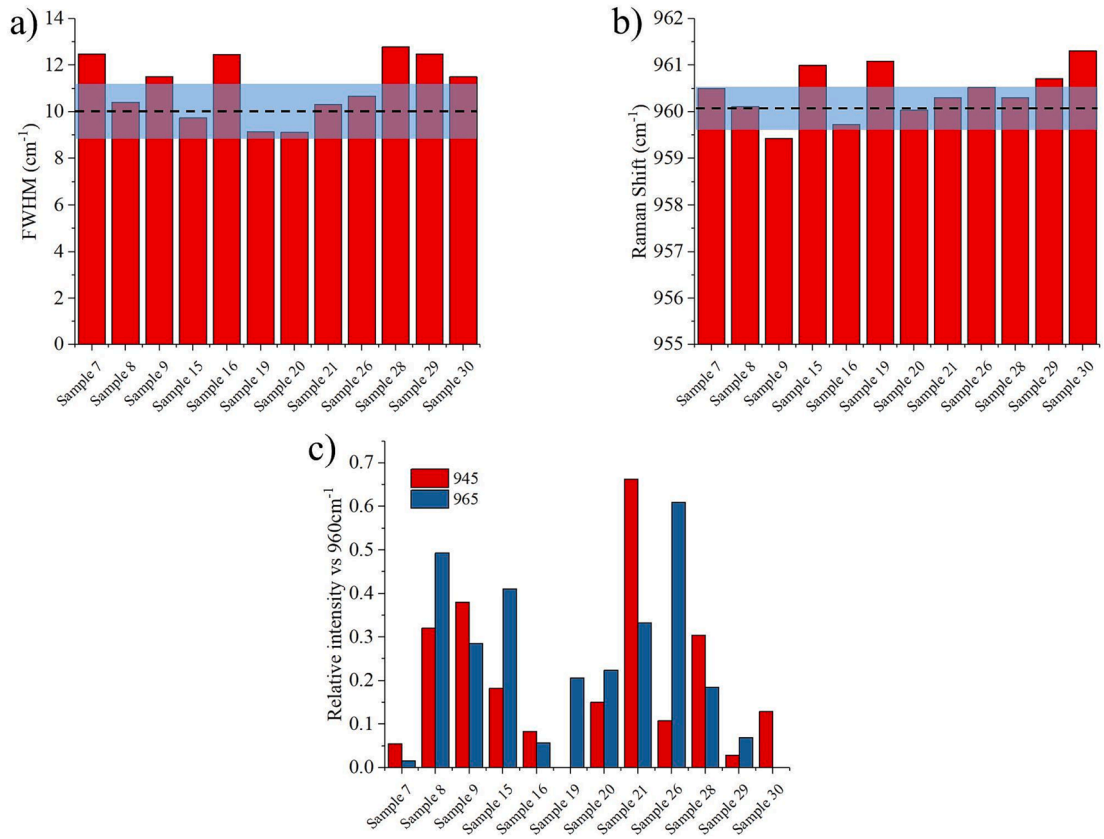

Fig. 7. Main spectroscopic parameters obtained from the different dentin specimens: (a) full-width half maximum of the 960 cm^{-1} band, (b) Raman shift of the 960 cm^{-1} band, (c) ratio between the intensity of the sub-bands at about 945 cm^{-1} and 965 cm^{-1} with respect to the main band at 960 cm^{-1}.

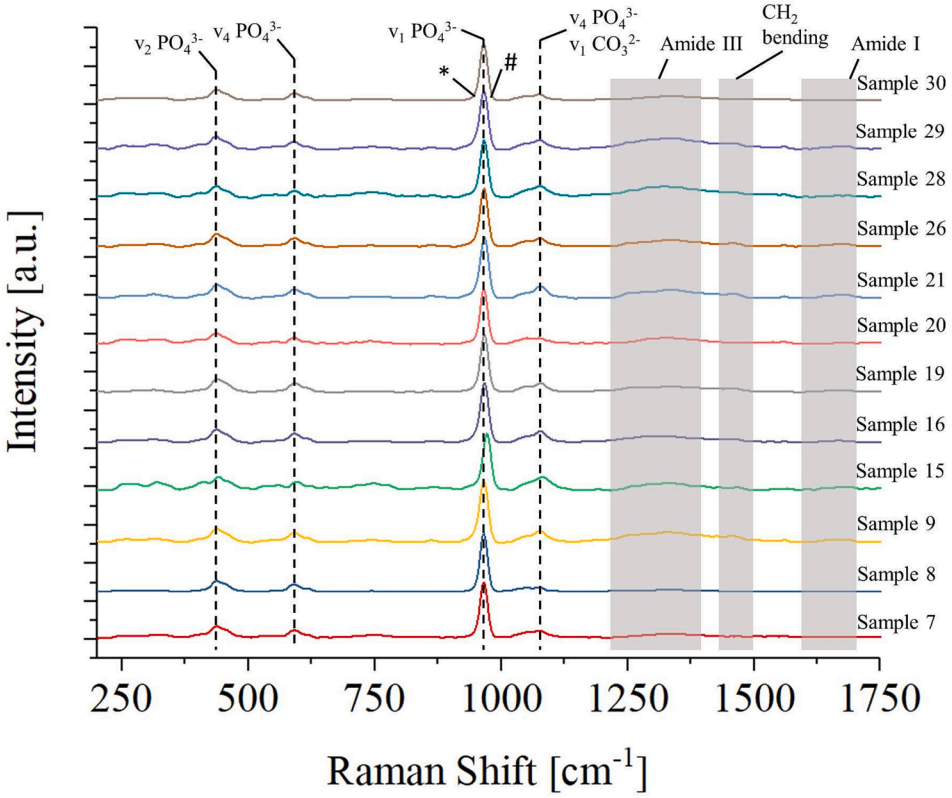

Fig. 8. Average Raman spectra as obtained on the enamel regions of the different specimens. Phosphate main vibration modes and regions related to Amide vibrations have been marked. Sub-bands at 945 and 975 cm^{-1} and related to distorted structures of PO_4^{3-} or CO_3^{2-} are marked with "*" and "#".

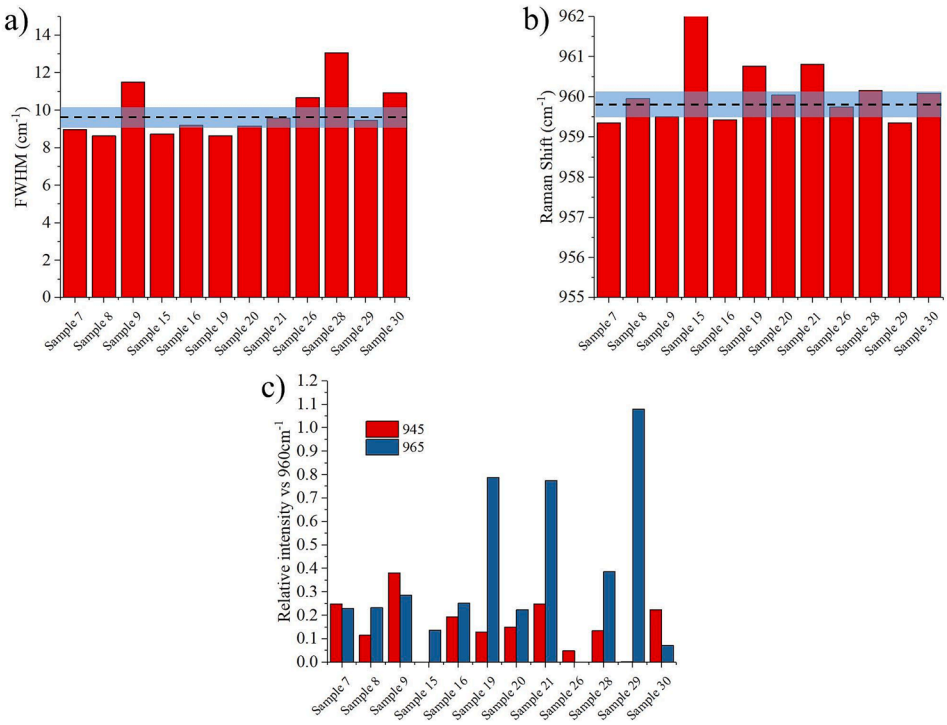

Fig. 9. Main spectroscopic parameters obtained from the different enamel specimens: (a) full-width at half maximum of the 960 cm^{-1} band, (b) Raman shift of the 960 cm^{-1} band, (c) ratio between the intensity of the sub-bands at about 945 cm^{-1} and 965 cm^{-1} with respect to the main band at 960 cm^{-1}.

were barely detectable. By evaluating the overall quantity of carbonate apatite, particularly the level of A-substituted apatite, it was feasible to estimate that three individuals (tombs no. 8, 20, and 26) were significantly younger than the others, while individuals from tombs no. 7, 16, 29, and 30 were potentially the oldest. All individuals, however, had reached skeletal maturity, which is indispensable to accurately assess biological sex through osteological analysis [5].

Nevertheless, the integration of osteological, archaeological, Raman, and proteomic data yielded highly confident estimations of biological sex and age for the discussed burials. Accurate sex estimation holds a pivotal role in archaeological theories, and our holistic approach minimizes the occurrence of "undetermined" classifications, a bias that often arises and limits archaeological interpretations. It is our hope that this pioneering research stimulates further discourse among archaeologists, chemists, biological anthropologists, and scientists in general, fostering the exploration of new potential techniques for sex and age estimation.

6. Ethical declaration

As researchers engaged in an archaeological-anthropological study on human remains within ancient tombs, we affirm our unwavering commitment to upholding the highest ethical standards, as endorsed by Squires et al. [26]. Our study is characterized by a profound respect for human dignity, cultural sensitivity, and collaboration with all relevant stakeholders. We steadfastly adhere to principles of scientific objectivity, ensuring the protection of data privacy and confidentiality, and recognizing human remains as subjects deserving of respect rather than objects of study.

In our dissemination efforts, we prioritize responsibility, emphasizing public outreach, education, and maintaining a tone of respectful communication. We remain accountable through the ethical review process and ongoing evaluation conducted by the Superintendence of Reggio Calabria and Vibo Valentia (permit no. 857/2022 and 885/2022-III/14, issued on April 13th, 2022). Our primary aim is to contribute to the advancement of knowledge while simultaneously preserving Cultural Heritage and fostering dialogues on the ethical considerations associated with the study of human remains.

7. Declaration of AI-assisted technologies

The graphical abstract of this work was partially generated by AI-assisted technology and further modified by the authors. No copyrights have been violated and the authors take full responsibility for the content of the publication.

CRediT authorship contribution statement

Enrico Greco: Conceptualization, Methodology, Formal analysis, Investigation, Writing – original draft, Writing – review & editing, Supervision, Project administration. **Andrea Maria Gennaro:** Conceptualization, Writing – original draft, Writing – review & editing, Project administration. **Dario Piombino-Mascali:** Formal analysis, Investigation, Writing – original draft, Writing – review & editing. **Daniela Costanzo:** Validation, Writing – review & editing, Project administration. **Simona Accardo:** Validation, Visualization, Writing – review & editing. **Sabina Licen:** Validation, Resources, Writing – review & editing. **Pierluigi Barbieri:** Methodology, Resources, Writing – review & editing. **Stefano Fornasaro:** Validation, Formal analysis, Writing – review & editing. **Sabrina Semeraro:** Validation, Writing – review & editing. **Elia Marin:** Methodology, Formal analysis, Investigation, Resources, Writing – original draft, Writing – review & editing. **Sara Signoretti:** Formal analysis, Investigation, Writing – review & editing. **Caterina Gabriele:** Formal analysis, Investigation, Writing – review & editing. **Marco Gaspari:** Methodology, Investigation, Resources, Formal analysis, Writing – review & editing.

Declaration of Competing Interest

The authors declare that they have no known competing financial interests or personal relationships that could have appeared to influence the work reported in this paper.

Data availability

Data will be made available on request.

Acknowledgments

The authors want to acknowledge the Director of the National Archaeological Museum of Reggio Calabria, Dr. Carmelo Malacrino, for his kind assistance, and Dr. Stephan N. Hassam for his valued suggestions. We also appreciate general support from the Italian Ministry of Culture and the Superintendence of Reggio Calabria and Vibo Valentia. We wish to express our gratitude to the Superintendence of Reggio Calabria and Vibo Valentia (SABAP) for loaning us figures no. 1 and 2, as well as to the National Archaeological Museum of Reggio Calabria (MArRC) for providing figures no. 3 and 4.

This work is dedicated to the memory of Dr. Donatella Capitani, who made significant contributions to Analytical Methodologies applied in Cultural Heritage studies, particularly those involving NMR techniques. She departed from us prematurely four years ago, and we continue to deeply miss her.

Appendix A. Supplementary data

Supplementary data to this article can be found online at https://doi.org/10.1016/j.microc.2023.109472.

References

[1] J. Hendy, F. Welker, B. Demarchi, C. Speller, C. Warinner, M.J. Collins, A guide to ancient protein studies, Nat. Ecol. Evol. 2 (2018) 791–799, https://doi.org/10.1038/s41559-018-0510-x.

[2] E. Greco, O. El-Aguizy, M.F. Ali, S. Foti, V. Cunsolo, R. Saletti, E. Ciliberto, Proteomic analyses on an ancient Egyptian cheese and biomolecular evidence of brucellosis, Anal. Chem. 90 (2018) 9673–9676, https://doi.org/10.1021/acs.analchem.8b02535.

[3] D. Tanasi, A. Cucina, V. Cunsolo, R. Saletti, A. Di Francesco, E. Greco, S. Foti, Paleoproteomic profiling of organic residues on prehistoric pottery from Malta, Amino Acids 53 (2021) 295–312, https://doi.org/10.1007/S00726-021-02946-4/FIGURES/3.

[4] F. Lugli, G. Di Rocco, A. Vazzana, F. Genovese, D. Pinetti, E. Cilli, M.C. Carile, S. Silvestrini, G. Gabanini, S. Arrighi, L. Buti, E. Bortolini, A. Cipriani, C. Figus, G. Marciani, G. Oxilia, M. Romandini, R. Sorrentino, M. Sola, S. Benazzi, Enamel peptides reveal the sex of the late antique 'lovers of Modena', Sci. Rep. 9 (2019) 13130, https://doi.org/10.1038/s41598-019-49562-7.

[5] T. White, P. Folkens, The human bone manual, Academic Press, San Diego (2005), https://doi.org/10.1016/C2009-0-00102-0.

[6] P.L. Walker, D.C. Cook, Gender and sex: vive la difference, Am. J. Phys. Anthropol. 106 (1998) 255–259, https://doi.org/10.1002/(SICI)1096-8644(199806)106:2<255::AID-AJPA11>3.0.CO;2-#.

[7] C. Hedenstierna-Jonson, A. Kjellström, T. Zachrisson, M. Krzewińska, V. Sobrado, N. Price, T. Günther, M. Jakobsson, A. Götherström, J. Storå, A female Viking warrior confirmed by genomics, Am. J. Phys. Anthropol. 164 (2017) 853–860, https://doi.org/10.1002/ajpa.23308.

[8] E. Andronico, Hypogaea. Tipologie edilizie, riti e corredi delle necropoli reggine di età ellenistica. Catalogo della mostra, Laruffa, Reggio Calabria, 2006.

[9] A. Gennaro, A. Candiano, G. Fargione, G. Mussumeci, M. Mangiameli, GIS and remote sensing for post-dictive analysis of archaeological features. A case study from the Etnean region (Sicily), Archeol. e Calc. 30 (2019) 309–328, https://doi.org/10.19282/ac.30.2019.18.

[10] T. Buonasera, J. Eerkens, A. de Flamingh, L. Engbring, J. Yip, H. Li, R. Haas, D. DiGiuseppe, D. Grant, M. Salemi, C. Nijmeh, M. Arellano, A. Leventhal, B. Phinney, B.F. Byrd, R.S. Malhi, G. Parker, A comparison of proteomic, genomic, and osteological methods of archaeological sex estimation, Sci. Rep. 10 (2020) 11897, https://doi.org/10.1038/s41598-020-68550-w.

[11] D. Taverna, M. Gaspari, A critical comparison of three MS-based approaches for quantitative proteomics analysis, J. Mass Spectrom. 56 (2021) 4669, https://doi.org/10.1002/jms.4669.

[12] N.A. Stewart, R.F. Gerlach, R.L. Gowland, K.J. Gron, J. Montgomery, Sex determination of human remains from peptides in tooth enamel, Proceed. Natl. Acad. Sci. 114 (2017) 13649–13654, https://doi.org/10.1073/pnas.1714926115.

[13] G.J. Parker, J.M. Yip, J.W. Eerkens, M. Salemi, B. Durbin-Johnson, C. Kiesow, R. Haas, J.E. Buikstra, H. Klaus, L.A. Regan, D.M. Rocke, B.S. Phinney, Sex estimation using sexually dimorphic amelogenin protein fragments in human enamel, J. Archaeol. Sci. 101 (2019) 169–180, https://doi.org/10.1016/J.JAS.2018.08.011.

[14] E. Marin, N. Hiraishi, T. Honma, F. Boschetto, M. Zanocco, W. Zhu, T. Adachi, N. Kanamura, T. Yamamoto, G. Pezzotti, Raman spectroscopy for early detection and monitoring of dentin demineralization, Dent. Mater. 36 (2020) 1635–1644, https://doi.org/10.1016/j.dental.2020.10.005.

[15] F.B. de Carvalho, A.F.S. Barbosa, F.A.A. Zanin, A. Brugnera Júnior, L. Silveira Júnior, A.L.B. Pinheiro, Use of laser fluorescence in dental caries diagnosis: a fluorescence x biomolecular vibrational spectroscopic comparative study, Braz. Dent. J. 24 (2013) 59–63, https://doi.org/10.1590/0103-6440201302123.

[16] P.G. Spizzirri, N.J. Cochrane, S. Prawer, E.C. Reynolds, A comparative study of carbonate determination in human teeth using Raman spectroscopy, Caries Res. 46 (2012) 353–360, https://doi.org/10.1159/000337398.

[17] E. Landi, A. Tampieri, G. Celotti, L. Vichi, M. Sandri, Influence of synthesis and sintering parameters on the characteristics of carbonate apatite, Biomaterials 25 (2004) 1763–1770, https://doi.org/10.1016/j.biomaterials.2003.08.026.

[18] A. Nanci, Ten Cate's oral histology: development, structure, and function, Mosby, St Louis, 2013.

[19] R. Ramakrishnaiah, G.U. Rehman, S. Basavarajappa, A.A. Al Khuraif, B.H. Durgesh, A.S. Khan, I.U. Rehman, Applications of Raman spectroscopy in dentistry: analysis of tooth structure, Appl. Spectrosc. Rev. 50 (2015) 332–350, https://doi.org/10.1080/05704928.2014.986734.

[20] A. Awonusi, M.D. Morris, M.M.J. Tecklenburg, Carbonate assignment and calibration in the Raman spectrum of apatite, Calcif. Tissue Int. 81 (2007) 46–52, https://doi.org/10.1007/S00223-007-9034-0.

[21] J. Shi, A. Klocke, M. Zhang, U. Bismayer, Thermally-induced structural modification of dental enamel apatite: decomposition and transformation of carbonate groups, Eur. J. Mineral. 17 (2005) 769–776, https://doi.org/10.1127/0935-1221/2005/0017-0769.

[22] B. Wopenka, J.D. Pasteris, A mineralogical perspective on the apatite in bone, Mater. Sci. Eng. C (2005) 131–143, https://doi.org/10.1016/j.msec.2005.01.008.

[23] T. Leventouri, A. Antonakos, A. Kyriacou, R. Venturelli, E. Liarokapis, V. Perdikatsis, Crystal structure studies of human dental apatite as a function of age, Int. J. Biomater. 2009 (2009), 698547, https://doi.org/10.1155/2009/698547.

[24] Y. Açil, A.E. Mobasseri, P.H. Warnke, H. Terheyden, J. Wiltfang, I. Springer, Detection of mature collagen in human dental enamel, Calcif. Tissue Int. 76 (2005) 121–126, https://doi.org/10.1007/s00223-004-0122-0.

[25] M.T. Kirchner, H.G.M. Edwards, D. Lucy, A.M. Pollard, Ancient and modern specimens of human teeth: a Fourier transform Raman spectroscopic study, J. Raman Spectrosc. 28 (1997) 171–178, https://doi.org/10.1002/(sici)1097-4555(199702)28:2/3<171::aid-jrs63>3.0.co;2-v.

[26] K. Squires, C.A. Roberts, N. Márquez-Grant, Ethical considerations and publishing in human bioarcheology, Am. J. Biol. Anthropol. 177 (2022) 615–619, https://doi.org/10.1002/ajpa.24467.